

Article

Biological Legacies and Rockfall: The Protective Effect of a Windthrown Forest

Maximiliano Costa ^{1,*}, Niccolò Marchi ¹, Francesco Bettella ¹, Paola Bolzon ¹, Frédéric Berger ²
and Emanuele Lingua ¹

¹ Department of Land, Environment, Agriculture and Forestry (TESAF), University of Padua, 35020 Legnaro, PD, Italy; niccolo.marchi@unipd.it (N.M.); francesco.bettella@unipd.it (F.B.); paola.bolzon@unipd.it (P.B.); emanuele.lingua@unipd.it (E.L.)

² Unité de Recherche Érosion Torrentielle, Neige et Avalanches (INRAE, UR ETNA), French National Research Institute for Agriculture, Food and the Environment, 38402 St-Martin-d'Hères, France; frederic.berger@inrae.fr

* Correspondence: maximiliano.costa@phd.unipd.it

Abstract: Windstorms represent one of the main large-scale disturbances that shape the European landscape and influence its forest structure, so post-event restoration activities start to gain a major role in mountainous forest management. After a disturbance event, biological legacies may enhance or maintain multiple ecosystem services of mountain forests such as protection against natural hazards, biodiversity conservation, or erosion mitigation. However, the conservation of all these ecosystem services after stand-replacing events could go against traditional management practices, such as salvage logging. Thus far, the impact of salvage logging and removal of biological legacies on the protective function of mountain stands has been poorly studied. Structural biological legacies may provide protection for natural regeneration and may also increase the terrain roughness providing a shielding effect against gravitational hazards like rockfall. The aim of this project is to understand the dynamics of post-windthrow recovery processes and to investigate how biological legacies affect the multifunctionality of mountain forests, in particular the protective function. To observe the role of biological legacies we performed 3000 simulations of rockfall activity on windthrown areas. Results show the active role of biological legacies in preventing gravitational hazards, providing a barrier effect and an energy reduction effect on rockfall activity. To conclude, we underline how forest management should take into consideration the protective function of structural legacies. A suggestion is to avoid salvage logging in order to maintain the multifunctionality of damaged stands during the recovery process.

Keywords: biological legacies; windstorm; rockfall activity; protection forests; natural disturbances; mountain forest management



Citation: Costa, M.; Marchi, N.; Bettella, F.; Bolzon, P.; Berger, F.; Lingua, E. Biological Legacies and Rockfall: The Protective Effect of a Windthrown Forest. *Forests* **2021**, *12*, 1141. <https://doi.org/10.3390/f12091141>

Academic Editor: Jean-Claude Ruel

Received: 15 July 2021

Accepted: 16 August 2021

Published: 24 August 2021

Publisher's Note: MDPI stays neutral with regard to jurisdictional claims in published maps and institutional affiliations.



Copyright: © 2021 by the authors. Licensee MDPI, Basel, Switzerland. This article is an open access article distributed under the terms and conditions of the Creative Commons Attribution (CC BY) license (<https://creativecommons.org/licenses/by/4.0/>).

1. Introduction

Mountain forests provide multiple services, from timber production to the protection of infrastructures against natural hazards like rockfall, landslides, or avalanches [1]. Considering the protective function, forests should always fulfill their role minimizing the risk exposure to local populations, therefore the interaction among natural hazards and mountain forests, as well as their management, has been widely studied [1–5]. Recently, rockfall research has been heading toward the study of simulation models [5–7], quantification of the protective effect of forests [5,8], and the influence of rockfall on the forest structure [9]. Natural disturbances (e.g., wildfires, windstorms, or insect outbreaks) may greatly affect the provision of ecosystem services by Alpine stands. Disturbances may undermine the mitigation effect that forests play as was observed after the windstorm Vivian in central Europe in the 1990s [10–12]. Moreover, natural disturbances are expected to increase in frequency and intensity in the coming years, especially in coniferous forests, mainly due to

climate change [13]. A correct forest management should consider natural disturbances in order to plan a rapid and efficient post-event restoration of a damaged area, in order to minimize the risk exposure and shorten the protection gap [12,14]. It is thus fundamental to recognize the role of biological legacies left by disturbances [15], since they can strongly influence both the post-disturbance recovery pattern [16,17] and the residual provision of ecosystem services through their type, number, and spatial arrangement. Regarding windstorms, the main disturbance affecting European forests [13,18–20], the main structural legacies that are present on a windthrown site are lying logs, stumps and snags, or snapped trees. After the Vivian storm in Switzerland, it was observed that the presence of deadwood could have a positive effect in scattering the energy of falling blocks, due to an increase of terrain roughness [21]. However, a quantification of this effect is still lacking, and it is not clear how long this effect may last. Although the wood decaying processes may decrease the protection provided by these material legacies over time [10], some studies suggest that lying logs may provide a barrier effect against snow and rocks even up to 30 years after the disturbance event [22]. In this paper, we present a case study of a protection forest located on the eastern Italian Alps. The target stand provided protection against rockfall until the 30 October 2018 when a massive windstorm, named Vaia, hit northern Italy, causing a loss of more than 10 million cubic meters of timber [23–25] and severely damaging the study site. This event modified the dynamics of interaction between the forested slope and rockfall events, hence the aim of this paper is to quantify the role played by biological legacies in providing a protective function in damaged protection forests. Results will allow to evaluate the effects of different post-disturbance management options, the first of which is salvage logging.

2. Materials and Methods

2.1. Study Area

The study site is located in the Dolomites, specifically on Monte Pore, close to Colcuc village (46°27′21″ N, 11°59′45″ E), municipality of Colle Santa Lucia, in Belluno province, NE Italy (Figure 1). The site is on a south-western slope and has an elevation ranging from 1360 to 1710 m a.s.l. The main forest species is Norway spruce (*Picea abies* (L.) Karst.), with the sporadic presence of European larch (*Larix decidua* Mill.) at higher elevations. On the 2 of April 2004, the site was affected by a massive landslide (around 4000 m³ of material) that defined the site as “active” for rockfall concern. The study site is crossed at different altitudes by a hiking/biking trail, a local, and a regional road. After the event, some concrete infrastructures and rockfall nets were built to minimize the risk for stakeholders (users of the trail and the local population). Some studies were started in the autumn of 2018 in order to evaluate and quantify the protective function of the forest stands of the area. However, on the 30 October 2018, the storm “Vaia” blew down most of the selected stands.

2.2. Field Data

2.2.1. Rockfall Activity

To simulate rockfall events and study their interaction with the protection forest, we used the probabilistic process-based model Rockyfor3D [26]. A field survey was conducted in summer 2018 in order to characterize the rockfall activity within the protection forest and to collect data required for the calibration of the rockfall model. Two transects were identified in the transit zone, one following the line of slope (vertical transect) and the other perpendicular to it (horizontal transect). The transects were 10 m wide and long enough to cover the entire length and width of the protection forest, equal to 440 and 175 m, respectively. Stakes were installed along the transects (one stake every 20–30 m) to aid relocation over time. The positions of the stakes were determined through RTK-DGPS measurements (TopCon HiPer V DGPS system, TopCon Positioning SRL, Tokyo, Japan). All the rockfall deposits within each transect and with one dimension (x, y or z) larger than 50 cm were measured. For each deposit we collected the three dimensions

of the block, using a measuring tape (± 1 cm), and its relative position with respect to a fixed georeferenced stake (horizontal distance and azimuth) using Trupulse 360 °B Laser Technology (Laser Technology Inc., Centennial, CO, USA). For each deposit we classified the rock's shape, using categories based on Dorren [26] and the stopping cause. The stopping cause must identify why an individual rock stopped at a certain location. The main causes may be classified using the object where the rock stopped, e.g., another rock, a tree, a lying log, a flat area, etc. It may also be classified as undefined when the stop is due to the total loss of kinetic energy. If the falling block was stopped by a tree, we also measured the tree DBH. In addition, for all the impacted trees within the transects, data on DBH, tree position, and characteristics (height and dimension) of the scars were recorded.

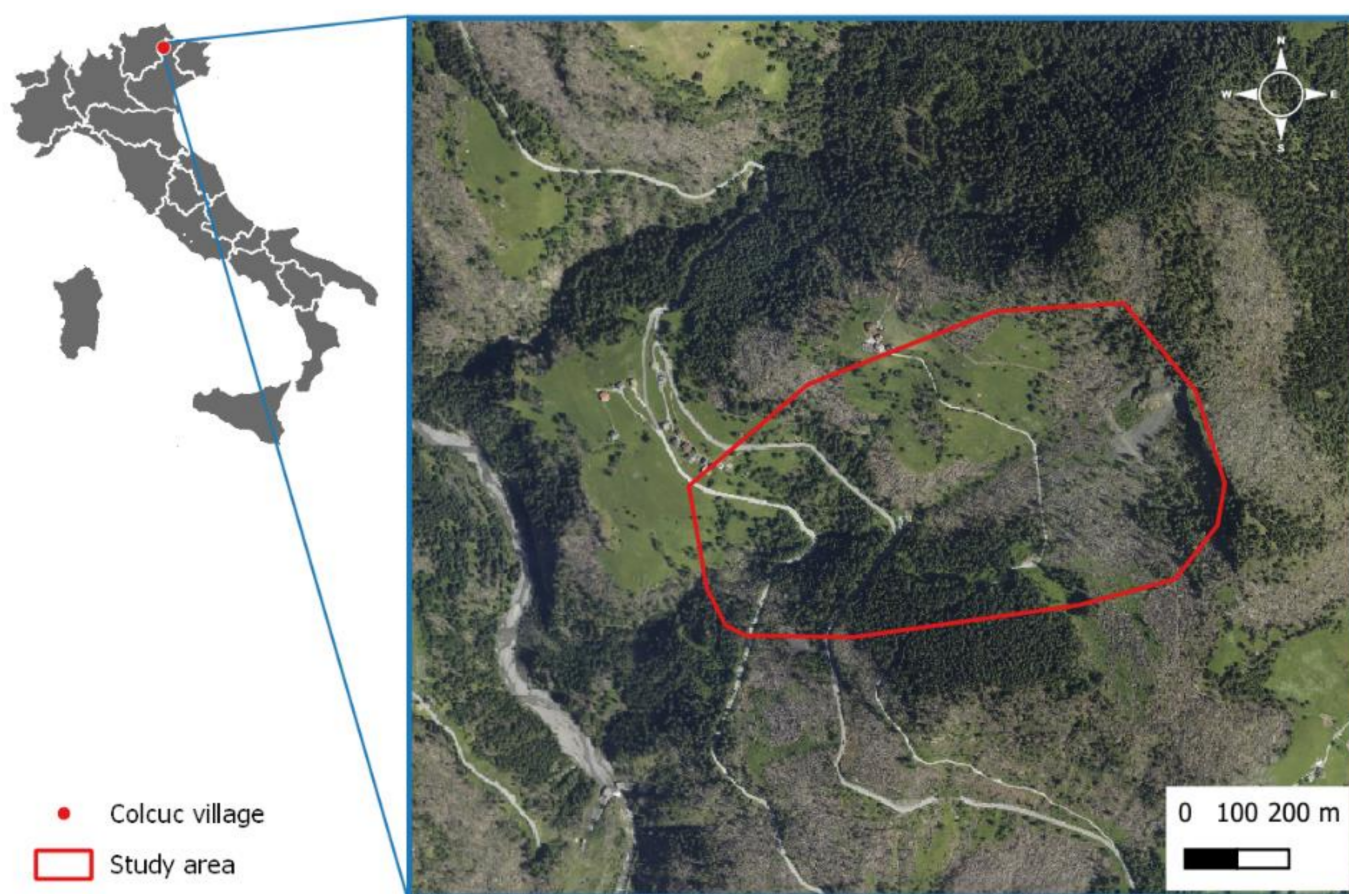


Figure 1. Location of the Colcuc study site, high-resolution orthoimagery from aerial surveys (acquired in 2019 by Veneto Region).

2.2.2. Slope Surface Parameters

To define ground and forest stand parameters required as input in the software package Rockyfor3D, field investigations were conducted during summer 2018, setting up 16 circular plots with a radius of 12 m (Figure 2). In each plot, we collected the position of the center (using a TopCon DGPS system, TopCon Positioning SRL, Tokyo, Japan). Within each plot, we recorded species, DBH, and relative position to the center for each tree with a DBH larger than 7.5 cm. We also collected the heights of the five trees closest to the center, in order to create a local tree height–diameter curve. For each plot, we evaluated the surface roughness (hereafter *RG*), expressed as the size of the material covering the slope's surface and assessing the three size probability classes named *rg70*, *rg20*, and *rg10*; these parameters are an expression of the different MOHs (Mean Object Heights, [27]). We recorded the main soil type for each plot following the classification provided in the Rockyfor3D Manual [26].

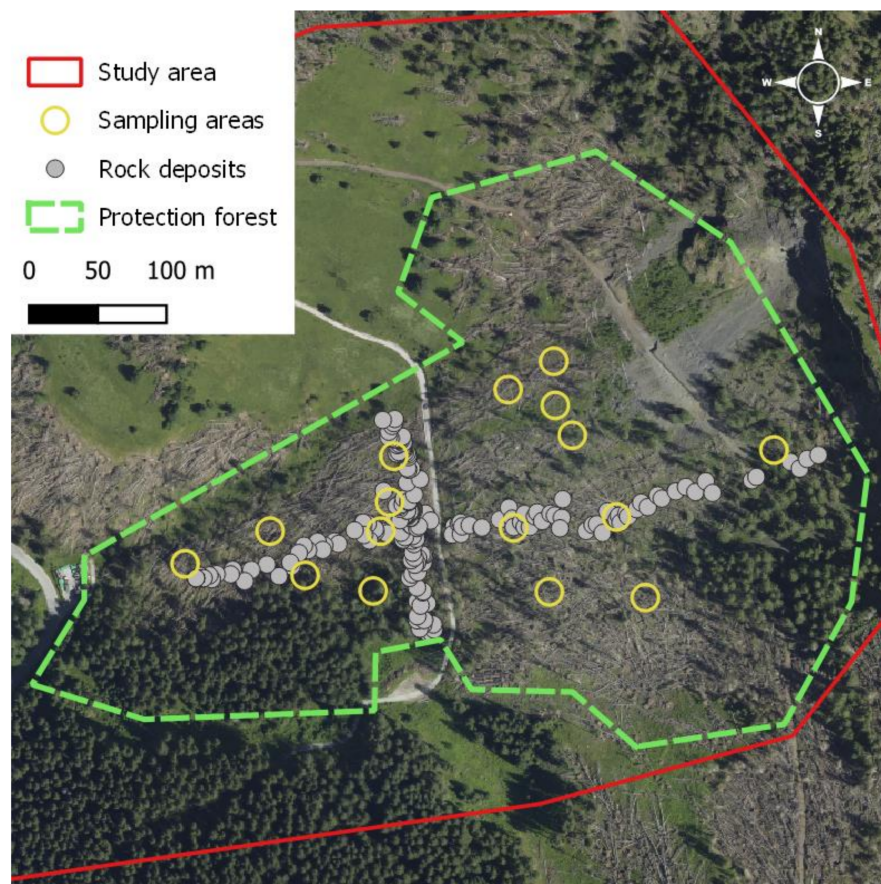


Figure 2. Localization of transects, surveyed rockfall deposits, and circular plots surveyed within the considered protection forest. High-resolution orthoimagery from aerial surveys (acquired in 2019 by Veneto Region).

2.3. Remote Sensing Data

The area has been flown over with different sensors both in pre-event and post-event conditions. A first campaign was performed by means of a high-density LiDAR scan in 2015 (appr. 12 pts/m²) and a UAV flight that provided high-resolution imagery and a Structure-from-Motion (SfM) point cloud. Because of the storm event, during 2019 the area was re-scanned with LiDAR sensor, adding a new very highly detailed data source (appr. 25 pts/m² for the study site).

2.4. Data Pre-Processing

Rockyfor3D simulations require a stack of raster layers with the same resolution and extent. For this specific purpose, the resolution has been set to a pixel size of 2 meters. The DTM (*dem.asc*) derived from the ground-classified point cloud collected during 2015 was used as a base layer. We selected the four roads crossing the study area as local checkpoints (calculation screens) to evaluate the number of passages and rock energy, while the conifer percentage (*conif_percent.asc*) and soil type (*soiltype.asc*) parameters were derived from field measurements and photo interpretation. Differently from the usual subdivision of the study area into subzones with homogeneous values, the RG files (*rg10.asc*, *rg20.asc*, and *rg70.asc*) were produced by hypothesizing a linear relation between slope and RG values measured in the field, offering a more realistic distribution across the site. We observed higher values of RG associated to lower values of slope, where we found a high presence of rock deposits. Finally, the file related to the position of trees (*treefile.txt*) was created by extracting the single tree locations using the software FINT V1 (ecorisq.org) (accessed on 17 October 2017) from the CHM derived from the SfM point cloud.

Post-Event Layers

All the input layers had to be updated to match the post-event configuration of the site. This required the delineation of the damaged area, in order to mask the windthrown areas and add the newly calculated input values. The damaged area was defined by the difference between CHMs, where all the areas with a decrease in height greater than 5 m have been considered as “damaged”, in order to avoid fine local bias from misaligned scans/pixels. If for the tree positions the update meant a simple difference, the *RG* layers had to be elaborated from scratch. The point cloud was filtered for first returns, height normalized on the DTM and then all the points above 2.5 m were removed. This height threshold was set according to the estimated most frequent maximum height of the downed material; the threshold value was verified on the field. Hence, in order to be consistent with the Rockyfor3D parameter, the *RG* values were calculated as the 10th, 20th, and 70th percentile of the points’ distribution starting from the maximum value (i.e., 2.5 m) to the lowest and then regularized according to the standard thresholds (see Manual’s Annex I [26]). Finally, to validate the new *RG* rasters, we collected in the field the values of *rg10*, *rg20*, and *rg70* at 103 different locations in the study area. Field sampled data and LiDAR data were compared in order to understand the pros and cons of both methodologies. For the statistical analysis, we used the free software PAST [28]. The rasters obtained through this methodology provides values of *RG* with a resolution of 2 m, allowing the interaction between falling blocks and deadwood to be investigated.

2.5. Simulations

The rockfall analysis was performed using Rockyfor3D [26], running 1000 simulations for each of the following scenarios:

- no forest (NFOR; reference): free-falling rocks; it is used to determine the potential energy, distance, and trajectory of rocks,
- with forest (FPRE; pre-event): rock falling under pre-event conditions, simulating the presence of the protection forest,
- with forest (FPOS; post-event): rock falling under post-event conditions, simulating the presence of biological legacies in the windthrown stand.

As concerns the other parameters that are necessary to the model, i.e., the shape of the test rock and its dimensions, these were based on the average size of rocks measured in the field. Rock density was set to 2700 kg/m³ (calcareous rock).

Ultimately, we set some checkpoints in order to collect data of passing rocks at different slope length from the hazard source. Each checkpoint collected mainly the number of rockfall passages, the kinetic energy of falling blocks, their velocity, and their passing heights. The position of checkpoints is shown in Figure 3.

2.6. Protective Effect

For the assessment of the protective effect of the stand (both standing and windthrown), we used the indices introduced by Dupire et al. [29]. The first index is the BARI (BARrier effect Index), it is computed using Formula (1) and is aimed at an assessment of the barrier effect of trees or lying logs (i.e., the capacity of stopping rocks in the transit zone). The second index is the MIRI (Maximum Intensity Reduction Index), it is computed using Formula (2) and assesses the reduction of kinetic energy due to the presence of trees or logs in the transit area (i.e., the loss of kinetic energy after impact with obstacles). The last one is the ORPI (Overall Rockfall Protection Index), it is computed using Formula (3) and quantifies the overall protection of the upslope stand.

$$BARI(x) = 100 \times \left(1 - \frac{N_{rock_{forest}}(x)}{N_{rock_{no-forest}}(x)} \right) \quad (1)$$

$$MIRI(x) = 100 \times \left(1 - \frac{E95_{forest}(x)}{E95_{no-forest}(x)} \right) \quad (2)$$

$$ORPI(x) = 100 \times \left(1 - \frac{\sum_{i=1}^{n_{forest}} E(x)}{\sum_{k=1}^{n_{no-forest}} E(x)} \right) \quad (3)$$

where, in Formula (1), $N_{rock_{forest}}(x)$ indicates the number of rocks that passed through a checkpoint in the FPRE, or FPOS, simulations, $N_{rock_{no-forest}}(x)$ indicates the number of rocks that passed through a checkpoint in the NFOR simulations. In Formula (2), $E95_{forest}(x)$ and $E95_{no-forest}(x)$, respectively, indicate the 95th percentile of kinetic energy of the rocks that passed through a checkpoint in the FPRE, or FPOS scenario and in the NFOR scenario.

In Formula (3), $\sum_{i=1}^{n_{forest}} E(x)$ indicates the total sum of the kinetic energy of each block that passed through a checkpoint in the FPRE, or FPOS, scenario, $\sum_{k=1}^{n_{no-forest}} E(x)$ refers to the NFOR scenario.

We computed the three indices for each checkpoint, for the FPRE and FPOS scenarios, using the NFOR scenario as the reference scenario. Considering the small sample size we applied the non-parametric Kolmogorov–Smirnov test to observe any difference among the three scenarios. For the statistical analysis we used the software PAST [28].

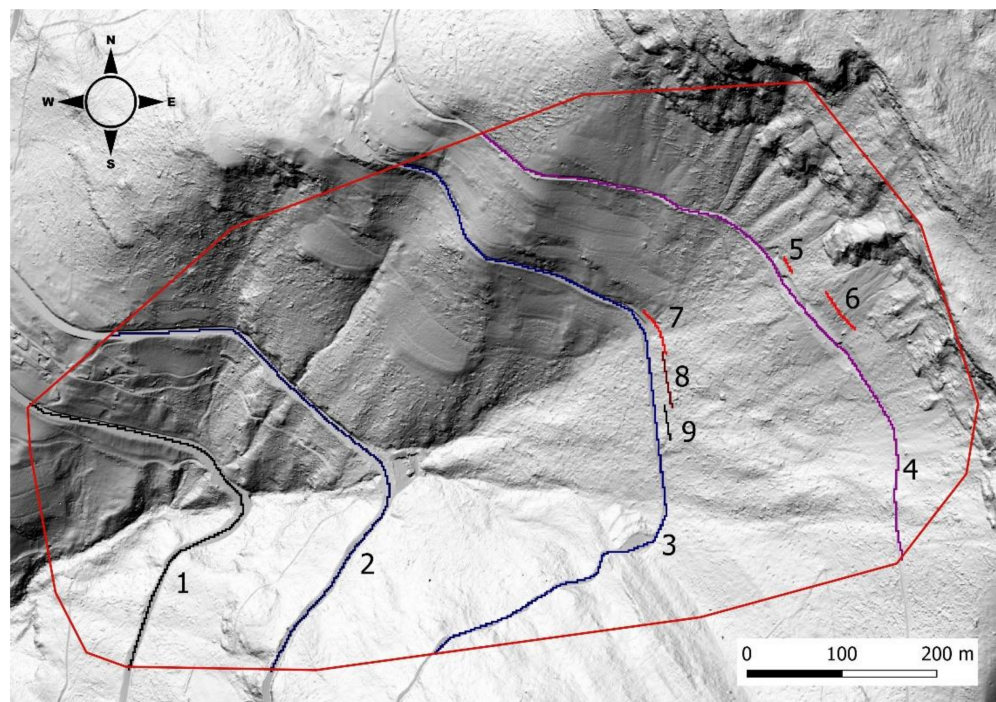


Figure 3. Position of the checkpoints used for computation of the indices. We identified the main roads, and the real nets present in the study area as checkpoints. The red line contours the study site, while the numbers indicate the ID of each checkpoint. High-resolution DTM from aerial surveys (acquired in 2019 by Veneto Region).

3. Results

3.1. Field Results

In the pre-Vaia forest stands, tree mean DBH was 30.5 cm with a standard deviation of 12.9 cm, the mean tree density was 720 trees/ha, and 100% were conifers. Inside the transects, we recorded 242 rocks with an average size of 1.5 m × 1.0 m × 0.8 m. The main stop cause (51% of cases) was classified as undefined, i.e., most of the rocks simply stopped due to the loss of their kinetic energy, 18% of rocks stopped on other rock deposits, 12%

stopped on stumps, 10% stopped on a tree and 9% stopped in a flat area. The shape of falling blocks was undefined (not relatable to any known geometric form) in the majority of the cases (48%), 26% were rectangular, 14% spheric and 12% discoid.

3.2. Validation of LiDAR Derived Roughness Values

The RG values collected in the field have been compared to the ones derived from the LiDAR point cloud (Figure 4). The field estimations were associated to the mean value of the LiDAR-derived raster cells that were within a circular area of 2 m radius.

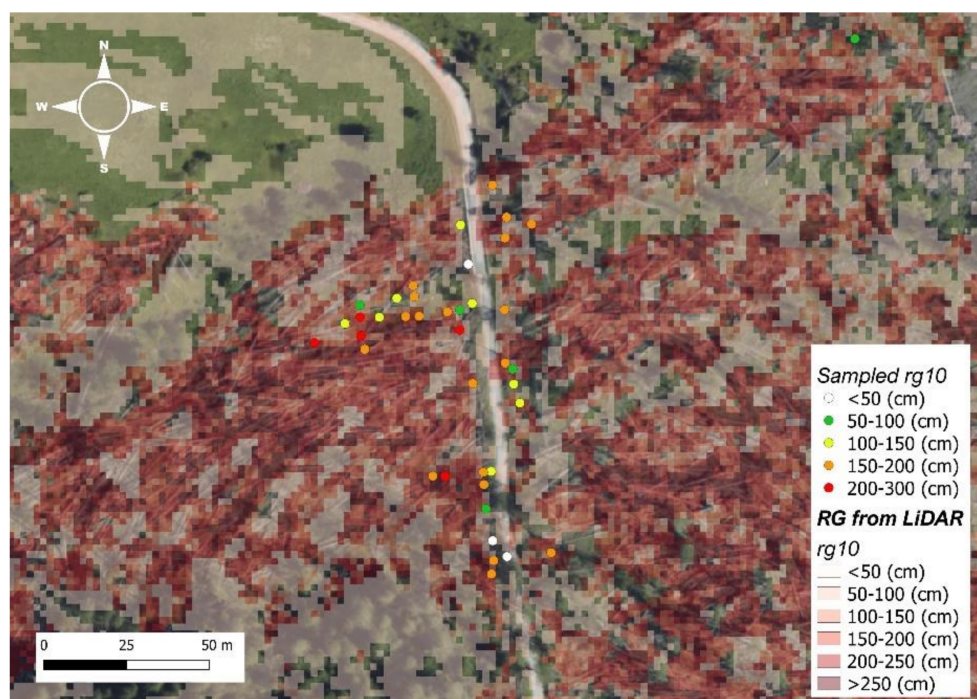


Figure 4. Comparison among roughness (rg_{10}) data extracted by LiDAR and sampled in the field. The map shows the spatialization of RG data obtained through a LiDAR source and of RG data sampled in the field.

After the removal of outliers, we compared rg_{10} values, we observed a mean value of 1.69 m for the sampled data and a mean value of 1.44 m for the LiDAR derived data. The average difference between the two sets of data (sampled data—LiDAR data) was 0.25 m, that is circa 30% of the smallest dimension of the average falling rock (see Section 3.1).

We did the same comparison for the rg_{20} : the mean value of sampled data was 1.06 m and the mean value of LiDAR derived data was 1.25 m, in this case the average difference between data was -0.18 m, 22.5% of the smallest dimension of the average falling rock.

Lastly, for rg_{70} we observed a mean value of sampled data of 0.70 m and a mean value of LiDAR-derived data of 0.64 m. The average difference resulted to be 0.06 m, in this case 7.5% of the smallest dimension of falling rocks.

Considering the acceptable difference among field collected data and LiDAR-derived raster and since it was a general underestimation leading to more conservative simulations (i.e., lower RG values), we adopted the LiDAR derived RG values for running the simulations in order to detect and take into account the spatial variability of windthrown material (Figure 5).

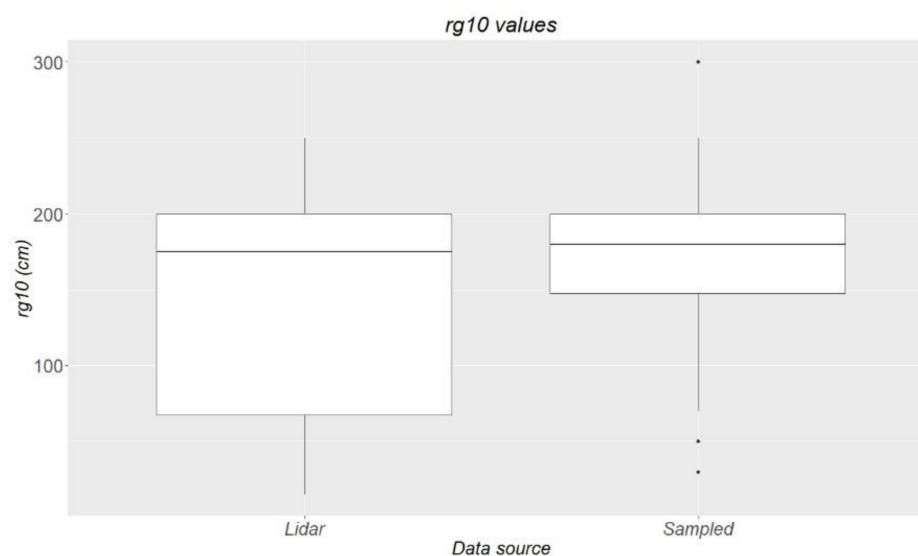


Figure 5. Comparison among roughness values ($rg10$) extracted by LiDAR and sampled in the field. The boxplot reports the results of the values obtained through the two methodologies.

3.3. Simulations Results

The results of the ‘no forest scenario’ show a potential severe rockfall activity in the study area, where falling rocks converge into a main gully, located in the center of the area.

The main source of activity is recognizable in the north-eastern part of the study area above the main trail and the roads where a rock cliff is located.

The first set of simulations, the NFOR scenario, show rockfall dynamics considering only the morphology of the study area, without taking into account the presence of trees or biological legacies. Simulation results are reported in Table 1.

Table 1. Summary of Rockyfor3D simulations outputs for the NFOR scenario. For each checkpoint, the table reports: n , the total number of registered passages of falling rocks; E_{95} , the 95th percentile of the energy of registered falling rocks; Ph_{95} , the 95th percentile of passing height values recorded at the checkpoint; V_{95} , the 95th percentile of the speed of recorded falling rocks.

Checkpoint	n (-)	E_{95} (kJ)	Ph_{95} (m)	V_{95} (m/s)
1	776,172	1080	1.3	20.3
2	586,053	953	2.6	20.0
3	2,796,600	1971	2.7	25.8
4	3,180,107	1843	4.0	26.1
5	192,933	1807	1.8	25.6
6	530,231	1984	1.9	26.3
7	1,216,722	2126	3.1	26.7
8	390,563	1969	2.8	25.3
9	606,256	1722	2.2	24.0

The highest rockfall activity was registered at checkpoint 4, the one closest to the source area. The registered number of passages was 3,180,107 with a 95th percentile of kinetic energy of 1843 kJ, a 95th percentile height of passage of 4.0 m and a 95th percentile of velocity of 26.1 m/s. It may be observed that increasing the distance from the source, so increasing the slope length, the number of rockfall passages decreases. On the other hand, the values of energy, passing height and velocity show less variability, mainly because we are reporting the 95th percentile.

The outputs of the simulation with forest data, FPRE scenario, show how rockfall activity interacted with the forest stand. Results show a reduction in the number of passages and a decrease in the mean kinetic energy of the falling block in the lower part of the main

catchment, where the forest is present. The energy and speed of falling blocks also show lower values if compared to the upper part, where tree density is lower (Table 2).

Table 2. Summary of Rockyfor3D simulations outputs in the FPRE scenario. For each checkpoint, the table reports: *n*, the total number of registered passages of falling rocks; E_95, the 95th percentile of the energy of registered falling rocks; Ph_95, the 95th percentile of passing height values recorded at the checkpoint; V_95, the 95th percentile of the speed of registered falling rocks.

Checkpoint	<i>n</i> (-)	E_95 (kJ)	Ph_95 (m)	V_95 (m/s)
1	478,121	816	0.9	17.1
2	490,779	578	1.3	15.7
3	1,523,292	1773	2.4	24.1
4	2,671,715	1733	4.1	25.3
5	191,329	1782	1.8	25.4
6	519,953	1965	1.9	26.2
7	792,383	1927	2.8	25.3
8	228,081	1787	2.5	23.9
9	141,892	1600	2.0	22.8

Regarding passing heights and velocity values, we can observe a reduction in most of the cases. Where the forest stand has a lower tree density, or where the forest is not present, Ph_95 and V_95 values remain constant.

Checkpoint 4 registered 2,671,715 passages with a 95th percentile of kinetic energy of 1733 kJ, a 95th percentile of passing heights of 4.1 m, and a 95th percentile of velocity of 25.3 m/s. While a reduction in the number of passages, kinetic energy and velocity may be observed, if compared to the NFOR scenario, Ph_95 does not show an appreciable change.

The outputs of the FPOS scenario shows the interaction of rockfall activity with the biological legacies of the damaged forest. In the upper part, where the forest had a lower density of trees, the number of passages and the energy of falling blocks are higher than in the lower part, where the forest stand had a higher density (Table 3).

Table 3. Summary of Rockyfor3D simulations outputs in the FPOS scenario. For each checkpoint, the table reports: *n*, the total number of registered passages of falling rocks; E_95, the 95th percentile of the energy of registered falling rocks; Ph_95, the 95th percentile of passing height values recorded at the checkpoint; V_95, the 95th percentile of the speed of registered falling rocks.

Checkpoint	<i>n</i> (-)	E_95 (kJ)	Ph_95 (m)	V_95 (m/s)
1	291,697	658	0.8	14.7
2	430,738	401	1.1	13.1
3	228,487	1140	1.5	20.0
4	901,333	1626	4.5	24.2
5	116,717	1537	1.5	23.9
6	464,749	1951	1.8	26.0
7	6492	2098	2.6	26.2
8	22,996	1839	2.4	24.1
9	1042	1819	1.9	24.1

The highest number of passages was always registered at checkpoint 4, where it was 901,333. In the same checkpoint, the registered E_95 and V_95 were 1626 kJ and 24.2 m/s, in both cases the values decreased if compared with the previous scenarios (NFOR and FPRE); the registered value of Ph_95 was slightly higher and was equal to 4.5 m.

The outputs of all the simulations are reported in Figure 6: it is possible to observe that the presence of deadwood influences the rockfall trajectories and the kinetic energy of falling blocks.

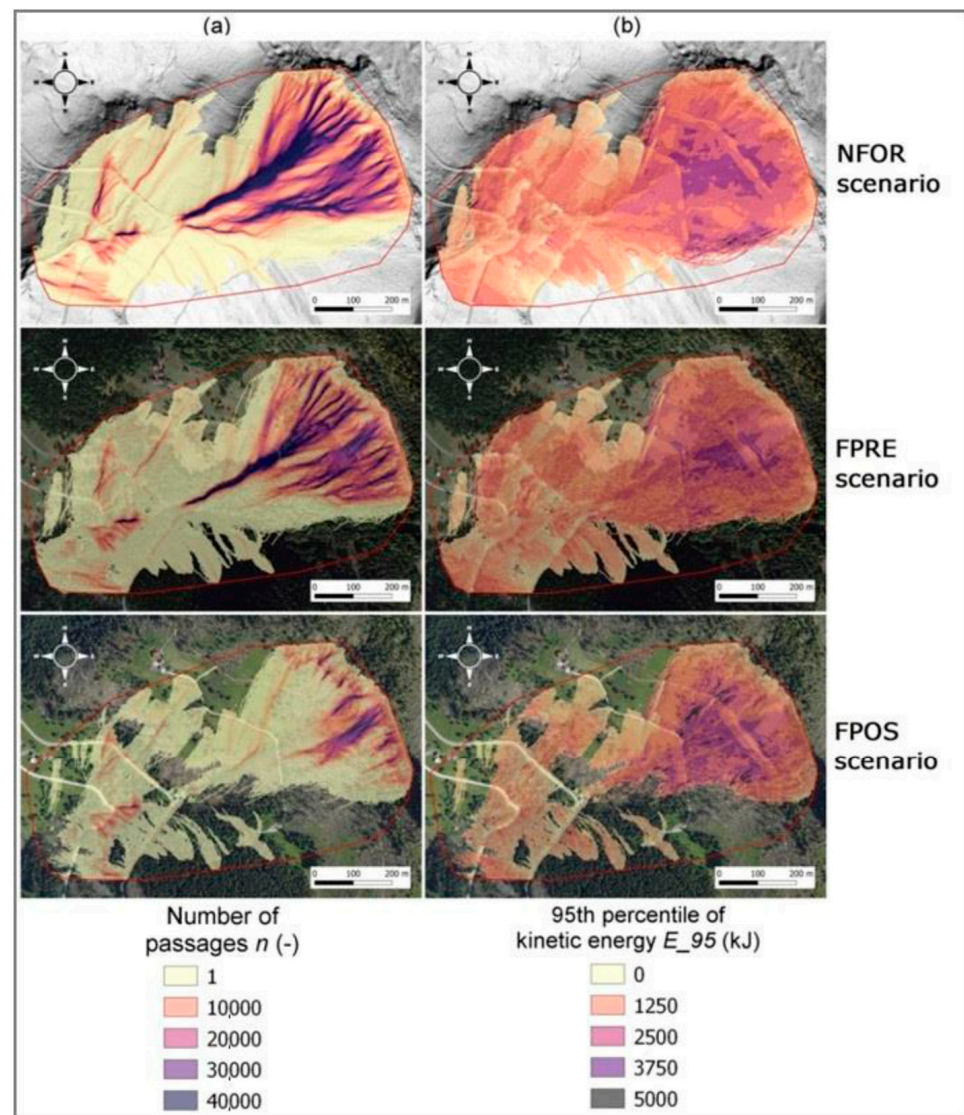


Figure 6. Output of Rockyfor3D simulations. In the first row the simulation in a ‘no forest’ scenario, in the second row the simulation in a ‘with forest’ scenario, in the third row the simulation in a ‘post windstorm’ scenario. Column (a) represents the number of passages of rockfall activity while column (b) represents the 95th percentile of the kinetic energy of falling blocks. The red line delimits the computational domain boundary of the numerical simulations.

3.4. Indices Computation

To evaluate and quantify the protective efficiency of the forest and the biological legacies against rockfall, we computed the Dupire’s indices [29] for the FPRE and FPOS scenarios, using NFOR scenario as a reference. The values of the indices are reported in Table 4, as well as the classification of the protective effect provided by the forested slope, both before and after the storm. These categories vary from Low Protective Effect to High Protective Effect [8] (as reported also in Figure 7). After the storm, there has been a clear increment in BARI, MIRI, and ORPI values. Considering the ORPI index and the protective efficiency (PE), in seven cases out of nine, we have an improvement from a lower protection class to a higher one (from low to medium and from medium to high).

Table 4. Summary of Dupire’s indices. For each checkpoint the table shows the results of the three indices computation, BARI, MIRI, ORPI for both the FPRE scenario and the FPOS scenario. The last column reports the classification of the protective efficiency (PE) of the forest stand according to the scenario (the categories are based on [8]).

Checkpoint	Scenario	BARI (-)	MIRI (-)	ORPI (-)	Classification
1	FPRE	38.4	24.4	52.6	Medium PE
	FPOS	62.4	39.1	76.0	Medium PE
2	FPRE	16.3	39.3	41.1	Low PE
	FPOS	26.5	57.9	59.8	Medium PE
3	FPRE	45.5	10.0	54.4	Medium PE
	FPOS	91.8	42.2	97.4	High PE
4	FPRE	16	6.0	26.4	Low PE
	FPOS	71.7	11.8	77.2	Medium PE
5	FPRE	0.8	1.4	2.4	Low PE
	FPOS	39.5	14.9	58.4	Medium PE
6	FPRE	1.9	1.0	3.1	Low PE
	FPOS	12.3	1.7	14.5	Low PE
7	FPRE	34.9	9.4	45.3	Low PE
	FPOS	99.5	1.3	99.6	High PE
8	FPRE	41.6	9.2	51.1	Medium PE
	FPOS	94.1	6.6	94.9	High PE
9	FPRE	76.6	7.1	78.9	Medium PE
	FPOS	99.8	−5.6	99.8	High PE

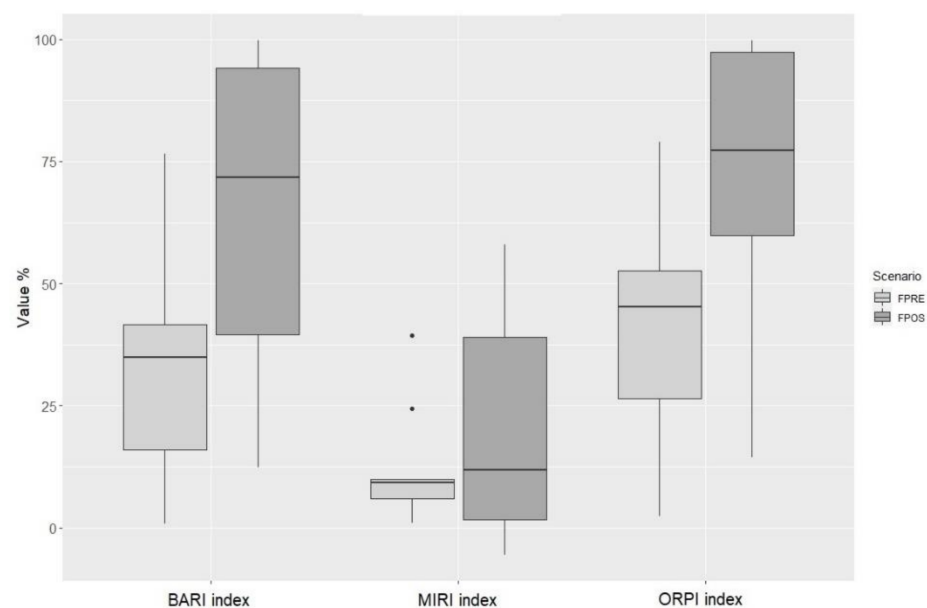


Figure 7. Boxplot of the values for the three indices BARI, MIRI, and ORPI in the scenarios FPRE, in light grey, and FPOS, in dark grey. The first index quantifies the barrier effect played by the protection forest, the second index is related to the maximum intensity reduction, and the last one is related to the overall protective effect.

Moreover, results show that lying logs mainly provide a barrier effect rather than an energy reduction of falling blocks. As can be observed in Figure 7, the variation among BARI indices is higher than the variation of MIRI indices. Kolmogorov–Smirnov test was used to compare the two scenarios (p -value ≤ 0.1): the difference between FPRE and FPOS is significant in the cases of BARI and ORPI indices. Instead, the MIRI indices do not present significant differences between the two scenarios.

4. Discussion

The role of a forested slope in the mitigation of rockfall hazard highlighted by the results of this study is aligned with the current literature [4,30–32]. We could observe and quantify the reduction of rockfall passages and their energy due to the presence of a protection forest, underlining the importance of these stands for risk assessment [5]. Moreover, our results provide an innovative detailed analysis of the impact of a windstorm on the protective efficiency of an alpine stand. Thanks to the use of indicators of protective efficiency [29], we have been able to compare how the interaction between a forested slope and rockfall hazard changed after a windthrow. Our results may help the understanding of the interaction of natural disturbances with the multifunctionality of mountain forests, a topic that is currently investigated in the literature, especially as concerns evaluation of the development of the provision of ecosystem services in a changing climate [33].

The results of the FPRE scenario show clearly that there is an effect of the forest in the reduction of the magnitude of rockfall activity. Figure 5 illustrates the barrier effect played by trees, as shown by the values of BARI and ORPI indices (Table 4). Moreover, concerning the kinetic energy of the falling blocks, the presence of the forest could lead to an energy reduction. Thanks to different positioning of the checkpoints, it was possible to evaluate the influence of the slope length on the magnitude of rockfall activity. According to the ORPI index, the forest stand varies from a low to a medium protective effect where the forested slope is longer. Our results also show that where the slope length is short the protection forest did not affect the passing heights of rocks.

Considering the FPOS scenario, the use of LiDAR-derived data represented an innovative way to study rockfall hazard. The methodology that we used for the creation of the *RG* rasters appeared to be efficient for a precise localization of biological legacies after the windstorm Vaia. Currently, remote sensing applications are starting to become more commonly used in forestry [34] and they may provide a high precision detection of biological legacies positions after a storm. The obtained *RG* rasters resulted as more accurate than data provided by field surveys: they present a better spatialization that leads to a good localization of lying logs. Moreover, during the surveys, we understood the difficulty of the estimation of *RG* values in the field. As a consequence, we think that the definition of a stricter procedure may avoid mistakes during the operations of data collection in the field.

The mean values of *RG* sampled in the field were slightly higher than LiDAR derived data. Consequently, the adoption of LiDAR derived *RG* as input for the numerical modelling provides a more conservative scenario. Using the raster produced with the LiDAR data we have been able to simulate the post windstorm scenario with high accuracy, considering the presence of biological legacies such as lying logs and stumps.

Moreover, the results of FPOS scenario show that the windthrown stand still provides an important protective function against rockfall. We expected this result considering previous studies that were carried out after other storms in the alpine area, e.g., Vivian or Lothar [12,21]. In addition, we observed that immediately after a windthrown event, the protective efficiency of the damaged stand is even higher than the previous forest, although the current literature affirms that the protective efficiency of a forested slope should start to decrease after a disturbance [12].

Our observations suggest that biological legacies, like lying logs, provide mainly a barrier effect rather than an energy reduction of falling blocks, as can be observed in Figure 6. The barrier effect played by deadwood has already been observed and analyzed by Fuhr et al. [35] and by Olmedo et al. [36]: the presence of lying logs significantly improves the surface roughness of a forested slope, in particular in a windthrown stand where all trees act like natural barriers on the ground.

Furthermore, biological legacies may provide a protective function against other gravitational hazards, for instance avalanches. In Switzerland it was observed that, after the storm Vivian, uncleared areas prevented avalanche release [10,12]. As concerns shallow landslides, it was observed that structural legacies cannot provide any protective effect,

mainly because the removal of the roots contribution to soil stability in windthrown areas may enhance the potential risk [12,37].

Knowing the spatial arrangements and conditions of deadwood, we could define the PE of the windthrown stand at different slope length level with a good accuracy. We observed an improvement of the PE for the majority of the checkpoints. This improvement of the protective role could last for a few years, before lying logs start to rot and the height of the logs from the ground starts to decrease, as observed in Wohlgemuth [12]. Moreover, with a reduction of deadwood height above the ground and with a higher portion of logs in direct contact with the soil, the wood decaying processes may accelerate [38], leading to lower protective efficiency of biological legacies.

Some empirical studies show that, after some branches breakage in the first years, the downslope movement of lying logs may be relatively small [10]. However, some tensile tests showed a reduction of the breaking point of logs, mainly due to the decay of wood. It was also observed that the level of decay was related to the microsite, mainly the height above ground of logs and their vegetation cover [39]; the presence of bark on logs may also influence the speed of decaying processes [40]. Although we were able to observe and quantify the protective role played by structural legacies, it is important to underline that this role is strictly connected with the type of disturbance that hit the protection forest. Other kinds of natural disturbances may create different biological legacies, with a different spatial arrangement, which may not provide the same barrier effect. For instance it was observed that after a wildfire, burnt logs and snags may behave in a different manner [41].

Furthermore the presence of biological legacies in a post-disturbance scenario, like a windthrown stand, may provide other important functions, from the protection of new seedlings [42,43], to the conservation of biodiversity and structural complexity of the forest [17,33,34]. The facilitation effect provided by deadwood can be fundamental for speeding up natural regeneration processes. The presence of biological legacies, indeed, may not only provide protection, but also create the condition for shortening the protection gap, which should be the main target of management strategies for a damaged protection forest [1,12,39].

The current literature investigates the impacts of traditional salvage logging practices, considering this management strategy as a second disturbance event [44–47] that can modify the provision of some ecosystem services. Our results may introduce a new element in the evaluation of the outcomes of this practice, suggesting that the removal of lying logs may eliminate the protective effect of the forested slope exposing infrastructures to rockfall hazard. Moreover, we would suggest adopting management strategies that aim to reach a resistant and resilient forest structure, considering (i) local environmental conditions, (ii) the multifunctionality of alpine forests, (iii) the interaction, and the possible future interactions of these stands with natural disturbances and climate change.

5. Conclusions

With this study, we evaluated the influence of structural biological legacies on rockfall activity after a windstorm in an alpine stand. After a natural disturbance, the protective function efficiency of a mountain forest may change drastically, and according to the severity of the event it may lead to a protection gap. However, we observed that in a short period of time after the event, the protective efficiency of the disturbed slope can be higher than before the event. This is because of lying logs and stumps, i.e., the structural biological legacies, which play an important role in providing a barrier effect against rockfall. Legacies' characteristics, and consequently the barrier effect, depend on the type of disturbance (e.g., wind). In addition, the time, or rather wood decay, is the other variable mainly affecting the protective function after a disturbance event, as observed in other studies [10,12,21,22]. We recommend that future research should focus on the protective role of structural biological legacies, considering other gravitational hazards, like shallow landslides and avalanches. Moreover, future studies should take into account the time

span of the protection gap, in order to understand when wood decaying processes will undermine the protection provided by deadwood on damaged slopes.

Finally, from an operative point of view, we would suggest avoiding traditional practices like salvage logging. Where a gravitational hazard is present, forest managers should consider other options with the target of enhancing the natural restoration of protection forests, in order to shorten the protection gap.

Author Contributions: Conceptualization, M.C., N.M., F.B. (Francesco Bettella) and E.L.; Methodology, M.C., N.M., F.B. (Francesco Bettella), P.B. and E.L.; Validation, M.C., Formal analysis, M.C.; Investigation, M.C. and F.B. (Francesco Bettella); Resources, E.L.; Data curation, M.C.; Writing—original draft preparation, M.C., N.M., F.B. (Francesco Bettella) and E.L.; Writing—review and editing, M.C., N.M., F.B. (Francesco Bettella), P.B., F.B. (Frédéric Berger) and E.L.; Visualization, M.C.; Supervision, E.L. All authors have read and agreed to the published version of the manuscript.

Funding: This research has been funded by the Interreg Alpine Space project “RockTheAlps” (ASP462), by Dept. TESAF, University of Padova in the framework of the project “Vaia FRONT” (CAVA_SID19_02), by the Veneto Region in the framework of the project Vaia-Land (OCDPC 558/2018), and by the Unione Montana Agordina and the University of Padova under the framework of InForTrac project (UNI-IMPRESA 2018).

Acknowledgments: We are grateful to M. Zampieri for field work, and N. Grasso, E. Belcore, P. Maschio, M. Piras for providing UAV data.

Conflicts of Interest: The authors declare no conflict of interest.

References

- Motta, R.; Haudemand, J.-C. Protective Forests and Silvicultural Stability. *Mt. Res. Dev.* **2000**, *20*, 180–187. [\[CrossRef\]](#)
- Brang, P. Resistance and elasticity: Promising concepts for the management of protection forests in the European Alps. *For. Ecol. Manag.* **2001**, *145*, 107–119. [\[CrossRef\]](#)
- Berger, F.; Quetel, C.; Dorren, L.K.A. Forest: A natural protection mean against rockfalls, but with which efficiency? *Interpraevent 2002 Pac. Rim Matsumoto Jpn.* **2002**, *2*, 815–826.
- Briones-Bitar, J.; Carrión-Mero, P.; Montalván-Burbano, N.; Morante-Carballo, F. Rockfall research: A bibliometric analysis and future trends. *Geosciences* **2020**, *10*, 403. [\[CrossRef\]](#)
- Moos, C.; Fehlmann, M.; Trappmann, D.; Stoffel, M.; Dorren, L. Integrating the mitigating effect of forests into quantitative rockfall risk analysis—Two case studies in Switzerland. *Int. J. Disaster Risk Reduct.* **2018**, *32*, 55–74. [\[CrossRef\]](#)
- Dorren, L.K.A. A review of rockfall mechanics and modelling approaches. *Prog. Phys. Geogr. Earth Environ.* **2003**, *27*, 69–87. [\[CrossRef\]](#)
- Moos, C.; Thomas, M.; Pauli, B.; Bergkamp, G.; Stoffel, M.; Dorren, L. Economic valuation of ecosystem-based rockfall risk reduction considering disturbances and comparison to structural measures. *Sci. Total Environ.* **2019**, *697*, 134077. [\[CrossRef\]](#)
- Dupire, S.; Bourrier, F.; Monnet, J.M.; Bigot, S.; Borgniet, L.; Berger, F.; Curt, T. The protective effect of forests against rockfalls across the French Alps: Influence of forest diversity. *For. Ecol. Manag.* **2016**, *382*, 269–279. [\[CrossRef\]](#)
- Moos, C.; Khelidj, N.; Guisan, A.; Lischke, H.; Randin, C.F. A quantitative assessment of rockfall influence on forest structure in the Swiss Alps. *Eur. J. For. Res.* **2021**, *140*, 91–104. [\[CrossRef\]](#)
- Frey, W.; Thee, P. Avalanche protection of windthrow areas: A ten year comparison of cleared and uncleared starting zones. *For. Snow Landsc. Res.* **2002**, *77*, 89–107.
- Schönenberger, W. Windthrow research after the 1990 storm Vivian in Switzerland: Objectives, study sites, and projects. *For. Snow Landsc. Res.* **2002**, *77*, 9–16.
- Wohlgemuth, T.; Schwitter, R.; Bebi, P.; Sutter, F.; Brang, P. Post-windthrow management in protection forests of the Swiss Alps. *Eur. J. For. Res.* **2017**, *136*, 1029–1040. [\[CrossRef\]](#)
- Seidl, R.; Thom, D.; Kautz, M.; Martin-Benito, D.; Peltoniemi, M.; Vacchiano, G.; Wild, J.; Ascoli, D.; Petr, M.; Honkaniemi, J.; et al. Forest disturbances under climate change. *Nat. Clim. Chang.* **2017**, *7*, 395–402. [\[CrossRef\]](#)
- Beghin, R.; Lingua, E.; Garbarino, M.; Lonati, M.; Bovio, G.; Motta, R.; Marzano, R. *Pinus sylvestris* forest regeneration under different post-fire restoration practices in the northwestern Italian Alps. *Ecol. Eng.* **2010**, *36*, 1365–1372. [\[CrossRef\]](#)
- Franklin, J.F.; Lindenmayer, D.; Macmahon, J.A.; Mckee, A.; Perry, D.A.; Waide, R.; Foster, D. Threads of Continuity: Ecosystem disturbance, recovery, and the theory of biological legacies. *Conserv. Pract.* **2000**, *1*, 8–17. [\[CrossRef\]](#)
- Johnstone, J.F.; Allen, C.D.; Franklin, J.F.; Frelich, L.E.; Harvey, B.J.; Higuera, P.E.; Mack, M.C.; Meentemeyer, R.K.; Metz, M.R.; Perry, G.L.W.; et al. Changing disturbance regimes, ecological memory, and forest resilience. *Front. Ecol. Environ.* **2016**, *14*, 369–378. [\[CrossRef\]](#)
- Lindenmayer, D.B.; Westgate, M.J.; Scheele, B.C.; Foster, C.N.; Blair, D.P. Key perspectives on early successional forests subject to stand-replacing disturbances. *For. Ecol. Manag.* **2019**, *454*, 117656. [\[CrossRef\]](#)

18. Gardiner, B.; Schuck, A.; Schelhaas, M.-J.; Orazio, C.; Blennow, K.; Nicoll, B. *Living with Storm Damage to Forests. What Science Can Tell Us 3*; European Forest Institute: Joensuu, Finland, 2013; ISBN 9789525980080.
19. Bebi, P.; Seidl, R.; Motta, R.; Fuhr, M.; Firm, D.; Krumm, F.; Conedera, M.; Ginzler, C.; Wohlgemuth, T.; Kulakowski, D. Changes of forest cover and disturbance regimes in the mountain forests of the Alps. *For. Ecol. Manag.* **2017**, *388*, 43–56. [[CrossRef](#)] [[PubMed](#)]
20. Forzieri, G.; Girardello, M.; Ceccherini, G.; Spinoni, J.; Feyen, L.; Hartmann, H.; Beck, P.S.A.; Camps-Valls, G.; Chirici, G.; Mauri, A.; et al. Emergent vulnerability to climate-driven disturbances in European forests. *Nat. Commun.* **2018**, *12*, 1081. [[CrossRef](#)] [[PubMed](#)]
21. Schönenberger, W.; Noack, A.; Thee, P. Effect of timber removal from windthrow slopes on the risk of snow avalanches and rockfall. *For. Ecol. Manag.* **2005**, *213*, 197–208. [[CrossRef](#)]
22. Rammig, A.; Fahse, L.; Bugmann, H.; Bebi, P. Forest regeneration after disturbance: A modelling study for the Swiss Alps. *For. Ecol. Manag.* **2006**, *222*, 123–136. [[CrossRef](#)]
23. Chirici, G.; Giannetti, F.; Travaglini, D.; Nocentini, S.; Francini, S.; D'Amico, G.; Calvo, E.; Fasolini, D.; Broll, M.; Maistrelli, F.; et al. Forest damage inventory after the “Vaia” storm in Italy. *For. Riv. Selvic. Ecol. For.* **2019**, *16*, 3–9. [[CrossRef](#)]
24. Cadei, A.; Mologni, O.; Röser, D.; Cavalli, R.; Grigolato, S. Forwarder productivity in salvage logging operations in difficult terrain. *Forests* **2020**, *11*, 341. [[CrossRef](#)]
25. Pellegrini, G.; Martini, L.; Cavalli, M.; Rainato, R.; Cazorzi, A.; Picco, L. The morphological response of the Tegnas alpine catchment (Northeast Italy) to a Large Infrequent Disturbance. *Sci. Total Environ.* **2021**, *770*, 145209. [[CrossRef](#)]
26. Dorren, L.K. A Rockyfor3D (v5.2) revealed—Transparent description of the complete 3D rockfall model. *ecorisQ Pap.* **2016**, *33*.
27. Dorren, L.K.A.; Berger, F.; Putters, U.S. Real-size experiments and 3-D simulation of rockfall on forested and non-forested slopes. *Nat. Hazards Earth Syst. Sci.* **2006**, *6*, 145–153. [[CrossRef](#)]
28. Hammer, O.; Harper, D.A.T.; Ryan, P.D. PAST—Palaeontological statistics, ver. 1.89. *Palaeontol. Electron.* **2009**, *4*, 1–9.
29. Dupire, S.; Bourrier, F.; Monnet, J.M.; Bigot, S.; Borgniet, L.; Berger, F.; Curt, T. Novel quantitative indicators to characterize the protective effect of mountain forests against rockfall. *Ecol. Indic.* **2016**, *67*, 98–107. [[CrossRef](#)]
30. Scheidl, C.; Heiser, M.; Vospernik, S.; Lauss, E.; Perzl, F.; Kofler, A.; Kleemayr, K.; Bettella, F.; Lingua, E.; Garbarino, M.; et al. Assessing the protective role of alpine forests against rockfall at regional scale. *Eur. J. For. Res.* **2020**, *139*, 969–980. [[CrossRef](#)]
31. Moos, C.; Dorren, L.; Stoffel, M. Quantifying the effect of forests on frequency and intensity of rockfalls. *Nat. Hazards Earth Syst. Sci.* **2017**, *17*, 291–304. [[CrossRef](#)]
32. Bianchi, E.; Accastello, C.; Trappmann, D.; Blanc, S.; Brun, F. The Economic Evaluation of Forest Protection Service Against Rockfall: A Review of Experiences and Approaches. *Ecol. Econ.* **2018**, *154*, 409–418. [[CrossRef](#)]
33. Irauschek, F.; Rammer, W.; Lexer, M.J. Evaluating multifunctionality and adaptive capacity of mountain forest management alternatives under climate change in the Eastern Alps. *Eur. J. For. Res.* **2017**, *136*, 1051–1069. [[CrossRef](#)]
34. Marchi, N.; Pirotti, F.; Lingua, E. Airborne and terrestrial laser scanning data for the assessment of standing and lying deadwood: Current situation and new perspectives. *Remote Sens.* **2018**, *10*, 1356. [[CrossRef](#)]
35. Fuhr, M.; Bourrier, F.; Cordonnier, T. Protection against rockfall along a maturity gradient in mountain forests. *For. Ecol. Manag.* **2015**, *354*, 224–231. [[CrossRef](#)]
36. Olmedo, I.; Bourrier, F.; Bertrand, D.; Berger, F.; Limam, A. Discrete element model of the dynamic response of fresh wood stems to impact. *Eng. Struct.* **2016**, *120*, 13–22. [[CrossRef](#)]
37. Bebi, P.; Bast, A.; Ginzler, C.; Rickli, C.; Schönggrundner, K.; Graf, F. Forest dynamics and shallow landslides: A large-scale gis-analysis. *Schweiz. Z. Forstwes.* **2019**, *170*, 318–325. [[CrossRef](#)]
38. Petrillo, M.; Cherubini, P.; Fravolini, G.; Marchetti, M.; Ascher-Jenuell, J.; Schärer, M.; Synal, H.A.; Bertoldi, D.; Camin, F.; Larcher, R.; et al. Time since death and decay rate constants of Norway spruce and European larch deadwood in subalpine forests determined using dendrochronology and radiocarbon dating. *Biogeosciences* **2016**, *13*, 1537–1552. [[CrossRef](#)]
39. Bebi, P.; Putallaz, J.M.; Fankhauser, M.; Schmid, U.; Schwitter, R.; Gerber, W. Die Schutzfunktion in Windwurfflächen. *Schweiz. Z. Forstwes.* **2015**, *166*, 168–176. [[CrossRef](#)]
40. Hagge, J.; Bässler, C.; Gruppe, A.; Hoppe, B.; Kellner, H.; Krah, F.S.; Müller, J.; Seibold, S.; Stengel, E.; Thorn, S. Bark coverage shifts assembly processes of microbial decomposer communities in dead wood. *Proc. R. Soc. B Biol. Sci.* **2019**, *286*, 20191744. [[CrossRef](#)]
41. Maringer, J.; Ascoli, D.; Dorren, L.; Bebi, P.; Conedera, M. Temporal trends in the protective capacity of burnt beech forests (*Fagus sylvatica* L.) against rockfall. *Eur. J. For. Res.* **2016**, *135*, 657–673. [[CrossRef](#)]
42. Marzano, R.; Garbarino, M.; Marcolin, E.; Pividori, M.; Lingua, E. Deadwood anisotropic facilitation on seedling establishment after a stand-replacing wildfire in Aosta Valley (NW Italy). *Ecol. Eng.* **2013**, *51*, 117–122. [[CrossRef](#)]
43. Wohlgemuth, T.; Kull, P.; Wüthrich, H. Disturbance of microsites and early tree regeneration after windthrow in Swiss mountain forests due to the winter storm Vivian 1990. *For. Snow Landsc. Res.* **2002**, *77*, 17–47.
44. Fischer, A.; Lindner, M.; Abs, C.; Lasch, P. Vegetation dynamics in Central European forest ecosystems (near-natural as well as managed) after storm events. *Folia Geobot.* **2002**, *37*, 17–32. [[CrossRef](#)]
45. Fischer, A.; Fischer, H.S. Individual-based analysis of tree establishment and forest stand development within 25 years after wind throw. *Eur. J. For. Res.* **2012**, *131*, 493–501. [[CrossRef](#)]

-
46. Taeroe, A.; de Koning, J.H.C.; Löf, M.; Tolvanen, A.; Heiðarsson, L.; Raulund-Rasmussen, K. Recovery of temperate and boreal forests after windthrow and the impacts of salvage logging. A quantitative review. *For. Ecol. Manag.* **2019**, *446*, 304–316. [[CrossRef](#)]
 47. Leverkus, A.B.; Buma, B.; Wagenbrenner, J.; Burton, P.J.; Lingua, E.; Marzano, R.; Thorn, S. Tamm review: Does salvage logging mitigate subsequent forest disturbances? *For. Ecol. Manag.* **2021**, *481*, 118721. [[CrossRef](#)]